

# Does the electrode amplification style matter? A comparison of active and passive EEG system configurations during standing and walking

Joanna E. M. Scanlon<sup>1</sup>  | Nadine Svenja Josée Jacobsen<sup>1</sup>  | Marike C. Maack<sup>1</sup> | Stefan Debener<sup>1,2,3</sup>

<sup>1</sup>Neuropsychology Lab, Department of Psychology, University of Oldenburg, Oldenburg, Germany

<sup>2</sup>Cluster of Excellence Hearing4all, University of Oldenburg, Oldenburg, Germany

<sup>3</sup>Center for Neurosensory Science and Systems, University of Oldenburg, Oldenburg, Germany

## Correspondence

Joanna E. M. Scanlon, Department of Psychology, Universität Oldenburg, D-26111 Oldenburg, Germany.  
Email: joanna.elizabeth.mary.scanlon@uni-oldenburg.de

## Funding information

Natural Sciences and Engineering Research Council of Canada, Grant/Award Number: PGSD3-519116-2018

## Abstract

It has been stated that active-transmission electrodes should improve signal quality in mobile EEG recordings. However, few studies have directly compared active- and passive-transmission electrodes during a mobile task. In this repeated measurement study, we investigated the performance of active and passive signal transmission electrodes with the same amplifier system in their respective typical configurations, during a mobile auditory task. The task was an auditory discrimination (1,000 vs. 800 Hz; counterbalanced) oddball task using approximately 560 trials (15% targets) for each condition. Eighteen participants performed the auditory oddball task both while standing and walking in an outdoor environment. While walking, there was a significant decrease in P3 amplitude, post-trial rejection trial numbers, and signal-to-noise ratio (SNR). No significant differences were found in signal quality between the two electrode configurations. SNR and P3 amplitude were test-retest reliable between recordings. We conclude that adequate use of a passive EEG electrode system achieves signal quality equivalent to that of an active system during a mobile task.

## KEY WORDS

attention, gait, mobile EEG, P3, signal quality, walking

## 1 | INTRODUCTION

Mobile EEG (electroencephalography) is becoming increasingly popular in cognitive neuroscience. This is because it allows us to begin studying brain activity in circumstances outside of typical controlled laboratory settings. These ambulatory experiments may be better able to describe the way the brain works in real life. However, movement can cause noise, which in turn can lead to negative effects on EEG

signal quality and statistical power (Boudewyn et al., 2018; Luck, 2014). It is, therefore, important to find solutions that facilitate good signal quality in mobile EEG acquisition.

Here we define noise as sources of variation in the collected data that are unrelated to the event-related potential (ERP) components measured (Luck, 2014). Non-neural noise, from both physiological and environmental sources, can have a large influence on the statistical power of EEG and ERP recordings (Boudewyn et al., 2018; Luck, 2014). Physiological

**Abbreviations:** EEG, electroencephalography; ERP, event-related potential; SNR, signal-to-noise ratio.

Editor: Pierfilippo De Sanctis

This is an open access article under the terms of the Creative Commons Attribution License, which permits use, distribution and reproduction in any medium, provided the original work is properly cited.

© 2020 The Authors. European Journal of Neuroscience published by Federation of European Neuroscience Societies and John Wiley & Sons Ltd

noise includes muscle activity, eye blinks, and movements, skin potentials, and cardiovascular activity (Gratton et al., 1983; Jung et al., 2000; Kappenman & Luck, 2010; Keil et al., 2014; Mathewson et al., 2017). Another source of EEG data noise is mechanical noise, which refers to artifacts that occur due to movement or locomotion, such as wire movements (Gwin et al., 2010; Symeonidou et al., 2018). The latter two types of noise are typically dealt with by restricting movements, and when this is not possible, advanced signal processing methods may be required. However, it is also possible that some particular EEG electrode features are more suitable for dealing with noise caused by mobile recordings than others.

Previous studies of electrode types tend to focus on the comparison between the use of active and passive signal transmission or amplification. Active-transmission electrodes use a small circuit board mounted on the electrode to pre-amplify signals directly on the surface of the scalp (i.e. pre-amplification) before passing these signals on to the amplifier (i.e. amplification), while passive electrodes simply collect the signals at the scalp which are then transmitted to the amplifier. Throughout this paper, we will use the terms “active” and “passive” to refer to whether signals were amplified at the scalp and amplifier (i.e. active-transmission) or only at the amplifier (i.e., passive-transmission), respectively. This pre-amplifier amplification at the scalp in active electrode configurations may help to achieve good signal quality by reducing detrimental effects of high impedance (Laszlo et al., 2014) and wire movements (Xu et al., 2017) on the data. Mobile passive electrode systems typically use a configuration with short wires that are fixed to the head and/or bundled together, as well as a small amplifier mounted directly on the head, in order to avoid the effects of wire movements (De Vos, Gandras, et al., 2014; De Vos, Kroesen, et al., 2014; Debener et al., 2012). While both of these configurations have been shown to collect laboratory quality EEG data during movement (De Vos, Gandras, et al., 2014; De Vos, Kroesen, et al., 2014; Debener et al., 2012; Scanlon et al., 2019, 2020) they have yet to be compared systematically using the same amplifier.

Laszlo et al. (2014) investigated differences between active and passive electrodes by having participants perform an auditory oddball task either with high or low impedance levels. They found that at low levels of electrode impedance ( $<2\text{ k}\Omega$ ) passive electrodes had better signal quality, with significantly lower levels of root-mean-squared (RMS) data noise. However, at higher impedance levels, active-transmission electrodes performed better, suggesting that, when application time is critical, active-transmission electrodes may be a good choice. A similar study by Mathewson et al. (2017) compared passive wet (with gel), active wet (with gel), and active dry (without gel) electrodes using the same amplifier. Active dry electrodes showed increased RMS data noise and

lower statistical power. Moreover, active and passive wet electrodes showed similar levels of data noise, with passive electrodes performing better at single-trial RMS data noise, and active wet electrodes having lower ERP data noise. These studies show some interesting differences between active and passive electrode systems, but they did not address the issue of movement during data recording.

Oliveira et al. (2016a, 2016b) had participants perform an auditory oddball task, while both sitting and walking on a treadmill, with three different electrode configurations: Biosemi wet (Active), Cognionics wet (Passive with active shielding), and Cognionics dry (Passive with active shielding). The wet systems outperformed the dry system, with the active system showing almost no statistical differences between the seated and walking conditions for all metrics, including prestimulus data noise, and signal-to-noise ratio (SNR). The wet systems also showed high test-retest reliability for prestimulus data noise during both conditions, but only the active-wet electrode system demonstrated high test-retest reliability in the SNR and P3 time window amplitude variance. However, this study used different amplifiers and electrode set-ups when comparing the active and passive electrode systems, and therefore it is not known whether electrode differences, amplifier differences or electrode set-up accounted for the observed results. Nathan and Contreras-Vidal, (2016) demonstrated negligible motion artifacts with active electrodes during a walking task at speeds up to 3 km/hr, with some evidence of motion artifacts at 4.5 km/hr. De Vos, Gandras, et al. (2014) and De Vos, Kroesen, et al. (2014) found no significant difference in single-trial data noise between sitting and walking during an oddball task, while using a passive electrode system and a head-mounted amplifier. Other studies have compared wet and dry electrode types, among which some of them (e.g. Kam et al., 2019; Marini et al., 2019; Mathewson et al., 2017) found that dry electrodes capture valid EEG signals. However, we are not aware of any reports evaluating the performance of dry electrodes during natural behavior (e.g., walking), other than Oliveira et al. (2016a, 2016b). Additionally, dual-electrodes consisting of an additional layer of mechanically coupled and inverted secondary electrodes which record only electrical noise and motion artifacts have also been used to effectively collect EEG data during mobile tasks (Nordin et al., 2018, 2019a, 2019b, 2019c). As of yet, there has not been a comparison study of active and passive electrode configurations during a mobile task using the same mobile EEG amplifier.

A task commonly used in studies evaluating mobile EEG systems is the auditory oddball task. Rare, task-relevant auditory events typically generate a P3 component, a positive deflection recorded approximately 250–500 milliseconds following a rare stimulus to which one has been asked to attend (Luck, 2014). The P3 component has been extensively studied, and can be observed reliably with low trial numbers, even

at the single-trial level (e.g. De Vos, Gandras, et al., 2014; De Vos, Kroesen, et al., 2014). The oddball task can also be used in a dual-task scenario to infer changes in attention, as attention to a primary task typically reduces the P3 amplitude to salient events in the secondary, oddball task (Polich, 1987; Polich & Kok, 1995). In previous mobile EEG studies, the auditory P3 component has been shown to decrease in amplitude by up to 30% during mobile dual-tasks such as walking (De Vos, Gandras, et al., 2014; De Vos, Kroesen, et al., 2014; Debener et al., 2012; Ladouce et al., 2019), cycling (Scanlon et al., 2019, 2020; Zink et al., 2016), and simulated driving (Chan et al., 2016) compared to the stationary oddball task. This has been interpreted in previous research to be because the mobile task takes attentional resources away from the oddball task, however research with animal models has suggested that this may be due to the inhibition of the auditory cortex by motion and motor system activation (Nelson et al., 2013; Nordin et al., 2019a, 2019b, 2019c; Otazu et al., 2009; Schneider et al., 2014). Interestingly, Ladouce et al. (2019) showed that simply being wheeled around without intentional movement was enough to significantly reduce the P3. The P3 has also been shown to be somewhat unique to individuals, as several studies have demonstrated test-retest reliability in P3 amplitude for different conditions (De Vos, Gandras, et al., 2014; De Vos, Kroesen, et al., 2014; Debener et al., 2012). The P3 reduction effect appears to be very robust, despite several of these studies using different EEG systems and demonstrating increases in measures of data noise such as SNR and data noise during walking (Debener et al., 2012) and biking (Scanlon et al., 2019; Zink et al., 2016).

The current study built on the body of mobile EEG and electrode comparison literature, and aimed to further understand how to best record EEG experiments in real-world circumstances. For mobile EEG studies, both active and passive electrodes require specific configurations according to their capabilities, and most EEG manufacturers do not have any system available that works identically with both active and passive electrodes. Therefore, this study reflects not only amplification style, but rather a comparison of the typical mobile active electrode configuration versus the typical mobile passive electrode configuration. Specifically, we aimed to learn whether there is a benefit to having pre-amplification that takes place on the head followed by amplification in a backpack (i.e. active electrode configuration), compared to a system using the same mobile amplifier, with highly restricted short wires and amplification only on the head (i.e. passive electrode configuration). In this experiment, participants performed two 6-min blocks of an auditory oddball task, while both standing and walking outdoors. ERP magnitude, morphology, and topography for the P3 were analyzed, as well as measures of prestimulus ERP data noise and SNR. In one session a passive electrode configuration was used, and in another session, an active electrode configuration was

used. Before exploring our main hypotheses, we intended to validate our measures by confirming that participants did not have significantly different cadences between walking conditions, and also showed significant differences in P3 amplitude between standards and targets in the oddball task. Our first hypothesis was that similar to previous studies, P3 amplitude would decrease during walking for both electrode types. The second hypothesis predicted that measures of data quality (i.e. post-trial rejection trial numbers, pre and post-trial rejection SNR and data noise) would also decrease due to increased noise in the walking condition. The third hypothesis predicted that an active electrode configuration would perform better in measures of post-trial rejection trial numbers, data noise, and SNR (both pre and post-trial rejection) than passive electrodes during movement. Finally, as our task involved collecting data from participants during standing and walking on two separate days, this offered the opportunity to quantify the test-retest reliability of P3 amplitudes and measures of data quality.

## 2 | METHODS

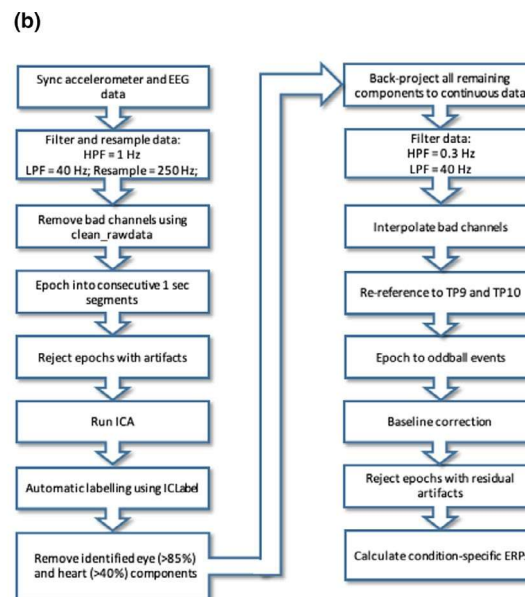
### 2.1 | Participants

Twenty-six individuals participated in the study, recruited through the Oldenburg University website. Data from seven participants were removed from the study due to technical issues during data collection. This was mainly due to problems in the wireless connection, which have since been addressed with the manufacturer and solved. Data from one participant were removed due to scheduling issues for the second appointment. This left 18 participants (mean age = 24; age range: 20–28; eight female) for the final analysis. Participants had no history of psychiatric or neurological problems and received an honorarium of 10 €/hour. Experimental procedures were approved by the Oldenburg University ethics committee.

### 2.2 | Materials

All participants came in for two separate recording sessions, approximately 3–15 (*Mean (M)* = 6) days apart, to record with each electrode type. Electrode type order was counterbalanced across participants. Recording time of day was within the same hour for 10 participants, and earlier/later times were counterbalanced according to electrode type in cases where the same time could not be scheduled for both sessions. For each experiment session, participants were fitted with an EEG cap with either active (actiCAP, EasyCap GmbH, Brain Products GmbH) or passive electrodes (EasyCap GmbH, Brain Products GmbH), each with identical 64 electrode

layouts. Ground and reference electrodes were embedded at the AFz and FCz (10–20 system) locations in the cap, respectively. The same two Brain Products LiveAmp amplifiers, which consisted of one amplifier for channels 1–32 and one for channels 33–64 (which were never switched), were used for all sessions. A Faros 180° eMotion (Mega Electronics, 2017) accelerometer sensor was fixed to the right foot of each participant using elastic tape. The auditory oddball task was presented using NBS (Neurobehavioral Systems) Presentation on a Dell (Latitude 5289) Ultrabook and earphones (Sony MDR-E9LP). Data were collected using the same Ultrabook, using LSL (Lab Streaming Layer) software to time-synchronously collect both the EEG channel data and the event markers from NBS Presentation. During *active* electrode sessions, the LiveAmp and Ultrabook were placed into a small backpack that was customized for the ventilation of the computer. All loose wires were tucked into the backpack to minimize wire movements. During *passive* electrode sessions, the LiveAmp was fixed to the top of the participant's head using elastic tape and a customized sponge that included holes to avoid any direct physical pressure on underlying electrodes (Figure 1a). The Ultrabook was also placed in the backpack for *passive* electrode sessions. At the beginning (and end) of each session, synchronization reference signals were sent into EEG and accelerometer data. To do this, the LiveAmp and Faros sensors were plugged into a sync-box after recordings were started and before they were stopped. Custom MATLAB scripts were used to offline prune the data streams into one synchronized data file. The experiment took place in an outdoor (roofed) basketball arena at the Oldenburg University campus. Pylons were placed in a rectangular formation around the whole arena and occasionally adjusted to avoid rain or excessive sunlight.



## 2.3 | Experiment set-up

Participants were asked to wash and dry their hair prior to the beginning of setup. During the EEG setup, gel was used to bridge the gap between the electrodes and the scalp. For active electrodes, SuperVisc High-Viscosity Electrolyte-Gel was used (according to Brain Products GmbH recommendations), and a blunt-tip syringe was used to mildly abrade the skin and move hair in order to adjust the impedance and connection. For passive electrodes, preparation started with alcohol applied using a cue tip, followed by the application of Abralyt HiCL Abrasive Electrolyte-Gel, also adjusted for impedance using a cue tip. Impedances were adjusted using Brain Vision Recorder software, with signals wirelessly sent from the LiveAmp to the Ultrabook. Impedance was adjusted to  $<10\text{ k}\Omega$  for each electrode. After preparation, all the needed equipment was moved to the outdoor arena for data recording. The experimenter then adjusted the audio volume to the participant's comfort level and began the recording.

## 2.4 | Experiment task and procedure

The whole experiment included three separate tasks; however, only one is described in the current study. Participants performed an auditory oddball task using headphones, while both standing next to a wall and walking around the arena (Figure 1a). In a third condition, participants walked with an experimenter; however, this will be described in a separate paper. During the *standing* condition, participants stood with their eyes open, staring at a brick wall. During the *walking* condition, participants walked at their own pace around the arena in a clockwise direction, following pylons as a guide.

**FIGURE 1** Conditions and pre-processing. (a): The four conditions used during the oddball task (staged image): Standing with active electrodes (top left), standing with passive electrodes (top right), walking with active electrodes (bottom left), walking with passive electrodes (bottom right). (b) Preprocessing pipeline used for all conditions

They were encouraged to keep a leisurely, slow pace in order to avoid aerobic effects.

Each condition block included an oddball task, in which participants were asked to silently count the number of deviant (target) tones. This included a set of 280 trials (15% deviants) plus 1–30 extra trials in order to keep the number of deviants unpredictable. Trial numbers before preprocessing were approximately equivalent between conditions (Standing Active:  $M_{\text{targ}} = 77.33$ , Standard deviation<sub>targ</sub> ( $SD$ ) = 3.68;  $M_{\text{stand}} = 508.22$ ,  $SD_{\text{stand}} = 13.07$ ; Standing Passive:  $M_{\text{targ}} = 77.94$ ,  $SD_{\text{targ}} = 3.84$ ;  $M_{\text{stand}} = 510.06$ ,  $SD_{\text{stand}} = 16.33$ ; Walking Active:  $M_{\text{targ}} = 79.17$ ,  $SD_{\text{targ}} = 3.29$ ;  $M_{\text{stand}} = 514.83$ ,  $SD_{\text{stand}} = 10.74$ ; Walking Passive:  $M_{\text{targ}} = 78$ ,  $SD_{\text{targ}} = 3.58$ ;  $M_{\text{stand}} = 514.11$ ,  $SD_{\text{stand}} = 12.78$ ). Additionally, the task was set to avoid playing two deviants subsequently. The tones were 800 and 1,000 Hz, and their standard (frequent) or target status was counterbalanced across participants. The inter-trial interval varied randomly between 500 and 1,500 ms (125 ms uniform distribution). This high variability was used in order to avoid a rhythm with which participants could synchronize their steps. Each block lasted approximately 5–6 min and was repeated twice for each condition, and counterbalanced. Participants reported the number of target tones counted to the experimenter at the end of each condition block.

## 2.5 | EEG preprocessing

Following data collection, EEG and accelerometer data were processed using EEGLAB 14.1.2b (Delorme & Makeig, 2004) and custom MATLAB scripts (Figure 1b). First, data from the accelerometer and EEG were synchronized using TTL pulses from the sync-box. The data were filtered with a high-pass filter (HPF; order 1650) of 1 Hz and low-pass filter (LPF; order 166) of 40 Hz, then resampled to 250 Hz. All filters were Hamming windowed, zero-phase finite impulse response (FIR) filters with a transition bandwidth at 25% of the lower passband edge (using EEGLAB function `pop_eegfiltnew`). Then, bad channels were removed using the function `clean_rawdata` (an EEGLAB wrapper function calling `clean_artifacts`), removing channels if they had a  $>5$ -s flatline, and  $<0.5$  correlation to a reconstruction of the channel based on other channels. These parameters were kept conservative in order to remove objective outliers and allow noise caused during the data collection to be processed and later analyzed. One channel was removed from two *active* (electrodes TP10, P5) and three *passive* (electrodes PO8, PO10, Fz) datasets across all subjects. Following this, data were epoched into consecutive 1-s segments, and epochs with artifacts (channel and global thresholds of 2 standard deviations) were removed. Extended infomax independent component analysis (ICA) as implemented in EEGLAB was then run on the remaining concatenated 1-s epochs and

ICLabel (Pion-Tonachini et al., 2019; see labeling.ucsd.edu) was used to identify and remove any components with over 85% probability of being eye-related or 40% probability of being due to heart activity (e.g. Viola et al., 2009). Then, all non-artifactual components were back-projected into continuous datasets, which were filtered with an HPF of 0.3 Hz (order 5500), and filtered again with an LPF of 40 Hz (order 166). The removed bad channels were then interpolated, and data were re-referenced to an average of TP9 and TP10. Data were then epoched to oddball events, beginning with the baseline 200 ms before the tone (at 0 ms) and ending 800 ms after the tone, creating 1-s epochs with 250 timepoints. Data were then baseline corrected from  $-200$  to 0 ms. Segments with remaining artifacts were removed, this time with channel and global thresholds of 3 standard deviations.

## 2.6 | Accelerometer preprocessing

Data collected from the right foot of each participant were used to determine cadence during the experiment. Right foot acceleration data (in mg's) were detrended and filtered with a low-pass filter of 30 Hz (2nd order Butterworth). A step detection algorithm was then used to mark step timing.

## 2.7 | Prestimulus data noise and SNR calculations

Prestimulus ERP data noise was calculated by first averaging data from the Pz electrode over all artifact-removed trials, then taking the standard deviation of all time-points in the  $-200$  to 0 ms interval before the tone onset, similar to previous studies (De Vos, Gandras, et al., 2014; De Vos, Kroesen, et al., 2014; Scanlon et al., 2017, 2019).

Signal-to-noise ratio (SNR) was calculated by first creating two ERPs per subject and condition, one for the even-numbered and one for the odd-numbered trials, and then taking the mean (i.e. signal) and the absolute difference (i.e. noise) between both (see Debener et al., 2007; Finneran et al., 2019; Kelly et al., 2014; Kremláček et al., 2012; Schimmel, 1967; Wright et al., 2011). The SNR was then obtained as the signal divided by the noise within the P3 time window for each subject. This procedure allows for measuring signal and noise at the same latency. SNR was then compared as an average for each subject between conditions. We were also interested in the effect of increasing trial numbers both without and with the factor of time, for our electrode and mobility conditions. Therefore, we plotted the SNR with increasing trial numbers both with time ignored by taking 100 trial permutations for each increasing number of trials and chronologically over time. We then performed the analysis using the final SNR value for each subject in each condition. To keep equal trial

numbers (within trial-rejection type) in each condition the SNR value was calculated at the minimum trial number (the number of trials for the subject with the fewest trials) in each condition.

## 2.8 | Statistical analysis

Data were analyzed using MATLAB (2016) custom scripts and JASP software (JASP Team, 2020). Cadence was assessed using a paired *t* test between the *walking* conditions of each electrode type. The P3 time window used was 284–484 ms, which was calculated by taking 100 ms before and after the average P3 peak time point for each subject and condition. This same time window was used for the SNR analysis. P3 amplitudes were computed by taking the mean of the P3 time window over all target trials for each participant (Luck, 2005a, 2005b). These values were then analyzed using repeated-measures  $2 \times 2 \times 2$  analyses of variance (ANOVA) with factors being electrode system (*active/passive*), mobile condition (*standing/walking*), and stimulus (standard/target), in order to first validate that the oddball task was performed correctly. Trial numbers and prestimulus data noise were analyzed using  $2 \times 2$  ANOVAs with factors being electrode type and mobile condition. Trial numbers, P3 amplitude, and SNR were analyzed using  $2 \times 2$  ANOVAs with the same factors, but using the target trials only. SNR pre and post-trial rejection, without and with time, were analyzed using repeated-measures  $2 \times 2 \times 2$  ANOVAs with factors being electrode system (*active/passive*), mobile condition (*standing/walking*), and trial rejection (*trial-rejected/non-trial rejected*). Effect sizes for  $p < .10$  ANOVA effects were calculated using the partial eta squared ( $\eta_p^2$ ). As a post hoc test of the null hypothesis for signal quality, Bayesian repeated-measures ANOVAs were carried out on the P3 amplitude, prestimulus data noise, and SNR. This analysis allows for the interpretation of evidence for or against the null hypothesis; therefore, offering us further information about whether the electrode types are effectively the same according to our measures. ANOVA tests were followed up with Holm-Bonferroni corrected (Abdi, 2010; Holm, 1979) paired *t* tests, only for results with significant (or marginal) group effects addressing our main research questions. Effect sizes for  $p < .10$  *t* tests were calculated using Cohen's *d* and 95% confidence intervals. Tests are considered significant at the level of  $\alpha = 0.05$ , unless otherwise stated, as in the case of Holm-Bonferroni corrected multiple *t* tests. Test-retest reliabilities were performed using an average value for each subject in each condition and were calculated as parametric (Pearson) correlations between electrode types for prestimulus data noise, SNR, and P3 amplitudes. These tests were then followed up with Shepherd's pi correlations, as the Shepherd's pi measure provides adequate statistical

power and protects against false positives due to outliers (Schwarzkopf et al., 2012). In the figures, distributions for prestimulus baseline noise and SNR were calculated using the rm\_raincloud function (modified by the authors; [https://github.com/RainCloudPlots/RainCloudPlots/tree/master/tutorial\\_matlab](https://github.com/RainCloudPlots/RainCloudPlots/tree/master/tutorial_matlab)). Shepherd's pi plots using Mahalanobis distance contours were created using Scatter Outliers (modified by the authors; Schwarzkopf et al., 2012) from the Shepherd toolbox.

## 3 | RESULTS

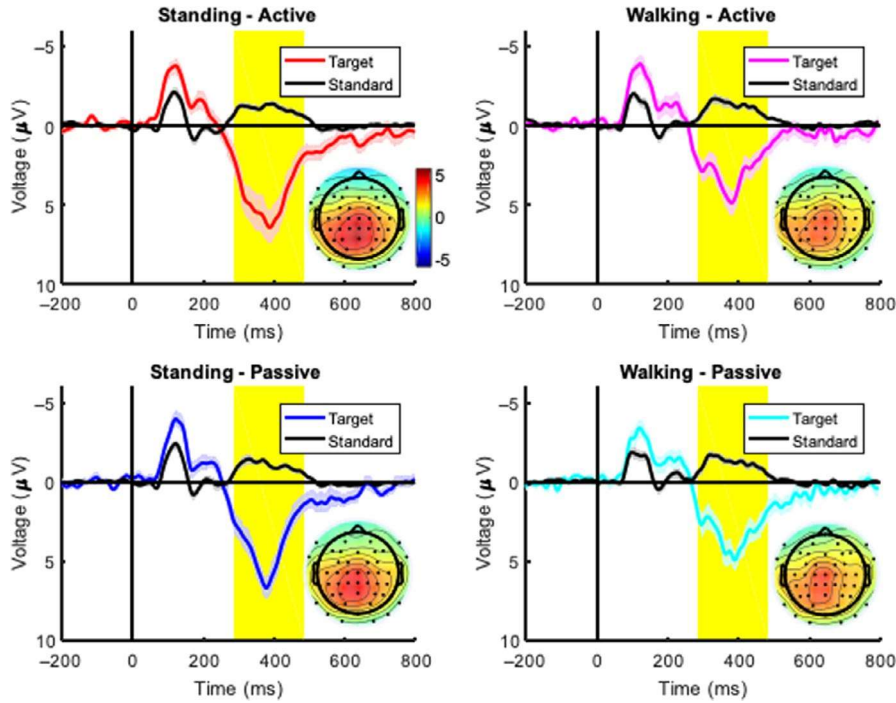
### 3.1 | Cadence

In order to validate that participants did not change their walking patterns in any systematic way, while using different EEG systems, we applied a step detection algorithm on the accelerometer right foot data to determine cadence (steps/minute) during the *walking* conditions. We found no significant difference in cadence between walking during *active* ( $M = 42.65$  steps/min) and *passive* ( $M = 44.20$  steps/min;  $M_{\text{diff}} = -1.55$ ;  $SD_{\text{diff}} = 6.46$ ;  $t(17) = -1.02$ ;  $p = .32$ ) electrode conditions.

### 3.2 | P3 Amplitude

ERP waveforms and P3 topographies are plotted in Figure 2. The highlighted regions in the plots illustrate a significant positive potential to the target stimuli peaking at approximately 385 ms. Inset maps also indicate that this potential had a posterior-central topography, as can be expected for a P3 component (De Vos, Gandras, et al., 2014; De Vos, Kroesen, et al., 2014; Debener et al., 2012). We investigated P3 amplitude by first performing a  $2 \times 2 \times 2$  ANOVA with factors of electrode system (*active/passive*), mobility (*standing/walking*) and stimulus (standard/target). Significant main effects of stimulus ( $F(1,17) = 69.52$ ;  $p < .001$ ;  $\eta_p^2 = 0.80$ ) and mobility ( $F(1,17) = 7.32$ ;  $p = .015$ ;  $\eta_p^2 = 0.30$ ) were found, but no main effect of electrode system ( $F(1,17) = 0.089$ ;  $p = .77$ ). Additionally, an interaction effect was found between mobility and stimulus ( $F(1,17) = 6.58$ ;  $p = .02$ ;  $\eta_p^2 = 0.28$ ). Target stimuli were most important in determining cognitive differences between the two mobility conditions, and were also used for the SNR analysis; therefore, these differences were further analyzed through a  $2 \times 2$  ANOVA using only the target trials. Here, we found again a significant main effect of mobility ( $F(1,17) = 7.72$ ;  $p = .013$ ;  $\eta_p^2 = 0.31$ ), due to larger amplitudes during the *standing* condition than the *walking* condition (Figure 2). There was no effect of electrode system ( $F(1,17) = 0.09$ ;  $p = .77$ ) or interaction ( $F(1,17) = 1.42$ ;  $p = .25$ ).

**FIGURE 2** Event-related potential (ERP) waveforms. Grand-average ERPs for each condition, computed at electrode Pz for both standard (black) and target (color/shades) conditions. Shaded regions indicate standard error of the mean. The P3 time window (284–484 ms) is highlighted. Scalp topographies show the grand-average of the P3 time window for target trials



To further investigate the patterns of P3 amplitude for the factors of electrode type and mobility, we followed up these results with a Bayesian ANOVA, including within-subject factor condition, using the same factors (Table 1). Here we found moderate evidence for the main effect of mobility ( $IBF = 4.97$ ), moderate evidence against the main effect of electrode system ( $IBF = 0.25$ ), and evidence against the interaction ( $IBF = 0.47$ ).

### 3.3 | Trial numbers

Table 2 shows the number of standard and target trials remaining after trial rejection for each condition. Analyzing

trial numbers allows us to estimate levels of data noise in each condition before trial rejection procedures (Oliveira et al., 2016a, 2016b). We calculated differences between trial numbers following trial rejection in repeated-measures  $2 \times 2$  ANOVA, with factors being electrode type (*active/passive*), and mobility (*standing/walking*), with target and standard trials added together. There was no main effect of electrode system ( $F(1,17) = 0.34; p = .57$ ), but a significant main effect for mobility ( $F(1,17) = 57.2; p = 7.77e-7; \eta_p^2 = 0.77$ ). This demonstrated that more trials were lost in the artifact rejection process during the *walking* ( $M = 451.14$ ; *range* = 374–515) conditions than the *standing* ( $M = 528.56$ ; *range* = 410–589) conditions. Additionally, there was no significant interaction effect between mobility and electrode type ( $F(1,17) = 1.43; p = .25$ ).

**TABLE 1**  $2 \times 2$  Bayesian repeated-measures ANOVA for P3 target amplitude (*mobility*: *standing* and *walking*; *electrode*: *active* and *passive*). “Models” column shows predictors included in each model. The “P(M)” column shows the prior model probability. The “P(M|data)” column shows the posterior model probability. The “BF<sub>M</sub>” column shows the posterior model odds, and the “BF<sub>10</sub>” column shows the Bayes factors of all models compared to the null model. The “error %” column shows estimates of the numerical error in the computation of the Bayes factor. All models are compared to the null model and are sorted from highest Bayes factor to the lowest

#### Bayesian repeated-measures ANOVA

##### Model comparison

Models	P(M)	P(M data)	BF <sub>M</sub>	BF <sub>10</sub>	Error %
Null model (incl. subject)	0.20	0.12	0.56	1.00	
Mobility	0.20	0.61	6.29	4.97	1.57
Mobility + electrode	0.20	0.16	0.76	1.30	2.52
Mobility + electrode + mobility × electrode	0.20	0.08	0.33	0.61	4.63
Electrode	0.20	0.03	0.13	0.25	0.91

*Note:* All models include subject.

Number of trials remaining after artifact rejection

Condition	Targets			Standards		
	Mean	Range	SD	Mean	Range	SD
Active standing	68.39	57–80	6.59	454.67	353–499	35.54
Passive standing	70.72	61–81	5.86	463.33	376–508	27.64
Active walking	60.44	50–71	5.80	391.89	330–433	26.99
Passive walking	58.11	45–71	6.71	391.83	328–444	28.68

### 3.4 | Prestimulus ERP data noise

Figure 3 (top) shows a distribution of the prestimulus data noise for each subject in each condition. The plot demonstrates an increase in data noise during *walking* compared to *standing*, but little difference between the electrode types. We used a  $2 \times 2$  ANOVA with factors of electrode system (*active/passive*), and mobility (*standing/walking*). Here we did not find a significant main effect of mobility ( $F(1,17) = 3.42$ ;  $p = .082$ ;  $\eta_p^2 = 0.17$ ), electrode ( $F(1,17) = 0.24$ ;  $p = .63$ ) or interaction ( $F(1,17) = 0.15$ ;  $p = .70$ ).

To further understand the patterns of prestimulus data noise for the factors of electrode type and mobility, we followed up these results with a Bayesian ANOVA, including within-subject factor condition, with the same factors (Table 3). The purpose of this second ANOVA was to investigate whether there was evidence in favor of the null hypothesis. Here we observed moderate evidence for the main effect of mobility ( $IBF = 3.24$ ), but moderate evidence against the main effect of the electrode ( $IBF = 0.26$ ) as well as against the interaction ( $IBF = 0.31$ ).

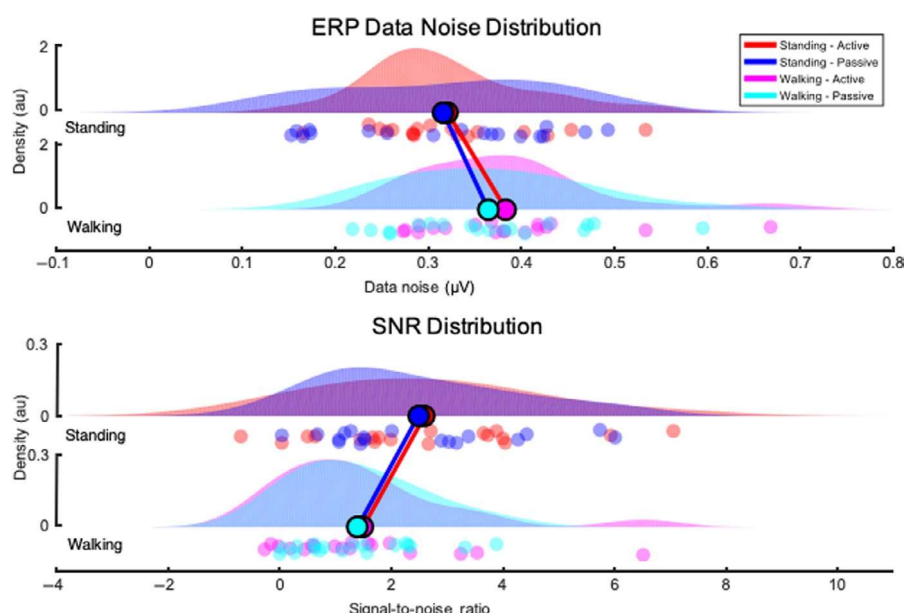


**TABLE 2** Trial numbers after artifact rejection

### 3.5 | Signal-to-noise ratio

Signal-to-noise ratio results for each subject and each condition are plotted as a distribution in Figure 3 (bottom). Evident from the plot is a decrease in SNR during the walking condition for both electrode configurations. We examined this using a  $2 \times 2$  ANOVA again with the factors electrode type (*active/passive*), and mobility (*standing/walking*). Here we again found a significant main effect of mobility ( $F(1,17) = 13.63$ ;  $p = .0018$ ;  $\eta_p^2 = 0.45$ ) and no effect of electrode system ( $F(1,17) = 0.14$ ;  $p = .71$ ) nor an interaction ( $F(1,17) = 0$ ;  $p = .98$ ).

In order to further understand the SNR patterns for the factors electrode system and mobility, we followed up these results with a Bayesian ANOVA, including within-subject factor condition, with the same factors (Table 4). Here we found strong evidence for the main effect of mobility ( $IBF = 159.36$ ) and moderate evidence against the main effect of electrode system ( $IBF = 0.25$ ) and the interaction ( $IBF = 0.31$ ).

We also were interested in whether this effect was held between both pre and post-trial rejection, as well as the effect of

**FIGURE 3** Data noise and signal-to-noise ratio (SNR) Distributions. Top: Distribution of ERP prestimulus data noise for each condition. Small dots under the distributions refer to single-subject values; larger dots refer to group means per condition. Density is scaled in arbitrary units and calculated using the MATLAB function ksdensity. Distribution here refers to the representation of how often each value on the x axis occurs within the data. Bottom: Distribution of signal-to-noise ratio for each condition

**TABLE 3**  $2 \times 2$  Bayesian repeated-measures ANOVA for ERP prestimulus data noise (*mobility*: standing and walking; *electrode*: active and passive). “Models” column shows predictors included in each model. The “P(M)” column shows the prior model probability. The “P(M<sub>l</sub>data)” column shows the posterior model probability. The “BF<sub>M</sub>” column shows the posterior model odds, and the “BF<sub>10</sub>” column shows the Bayes factors of all models compared to the null model. The “error %” column shows estimates of the numerical error in the computation of the Bayes factor. All models are compared to the null model and are sorted from highest Bayes factor to the lowest

Bayesian repeated-measures ANOVA					
Model comparison					
Models	P(M)	P(M <sub>l</sub> data)	BF <sub>M</sub>	BF <sub>10</sub>	Error %
Null model (incl. subject)	0.20	0.18	0.85	1.00	
Mobility	0.20	0.57	5.29	3.24	1.67
Mobility + electrode	0.20	0.16	0.76	0.91	8.44
Mobility + electrode + mobility × electrode	0.20	0.05	0.20	0.28	1.98
Electrode	0.20	0.05	0.19	0.26	0.73

Note: All models include subject.

**TABLE 4**  $2 \times 2$  Bayesian repeated-measures ANOVA for SNR (*mobility*: standing and walking; *electrode*: active and passive). “Models” column shows predictors included in each model. The “P(M)” column shows the prior model probability. The “P(M<sub>l</sub>data)” column shows the posterior model probability. The “BF<sub>M</sub>” column shows the posterior model odds, and the “BF<sub>10</sub>” column shows the Bayes factors of all models compared to the null model. The “error %” column shows estimates of the numerical error in the computation of the Bayes factor. All models are compared to the null model and are sorted from highest Bayes factor to the lowest

Bayesian repeated-measures ANOVA					
Model comparison					
Models	P(M)	P(M <sub>l</sub> data)	BF <sub>M</sub>	BF <sub>10</sub>	Error %
Null model (incl. subject)	0.20	0.01	0.02	1.00	
Mobility	0.20	0.82	17.83	159.36	35.63
Mobility + electrode	0.20	0.14	0.63	26.41	1.81
Mobility + electrode + mobility × electrode	0.20	0.04	0.17	8.09	2.39
Electrode	0.20	0.001	0.01	0.25	0.95

Note: All models include subject.

increasing trial numbers without the factor of time. Figure 4a demonstrates SNR computed and plotted with increasing trial numbers for each condition, for trials before and after trial-rejection. Evident from the plot is a small SNR benefit with increasing trial numbers, as well as lower SNR overall in the walking conditions. We then quantified this effect using a  $2 \times 2 \times 2$  ANOVA on the final SNR value in each condition. We found here a significant main effect of mobility ( $F(1,17) = 13.29$ ;  $p = .002$ ;  $\eta p^2 = 0.44$ ) but not for electrode configuration ( $F(1,17) = 0.63$ ;  $p = .44$ ). There was also a main effect of pre/post-trial rejection ( $F(1,17) = 18.90$ ;  $p < .001$ ;  $\eta p^2 = 0.53$ ), with larger SNR for the pre trial-rejected data. There were no significant interaction effects (all  $F$ 's  $< 4$ ).

Additionally, we were interested in whether trial rejection has an impact on SNR over time. Figure 4b demonstrates SNR computed and plotted with increasing trial numbers in chronological order for each condition, for trials before and after trial-rejection. Evident from the plots, the SNR benefit

of increasing trials appears to level off after approximately 40 trials in each condition. In order to quantify this effect, we performed a  $2 \times 2 \times 2$  ANOVA on the final SNR value in each condition. There was a significant main effect for mobility ( $F(1,17) = 15.63$ ;  $p = .001$ ;  $\eta p^2 = 0.479$ ), but no significant effect for electrode system ( $F(1,17) = 0.94$ ;  $p = .35$ ) or pre/post-trial rejection ( $F(1,17) = 0.42$ ;  $p = .53$ ) or any interaction (all  $F$ 's  $< 1$ ).

### 3.6 | Test-retest reliability

Test-retest reliability between electrode types for prestimulus ERP noise, SNR, and P3 amplitude were measured using correlations and followed up with Shepherd's pi correlations. Figure 5 depicts these correlations. Prestimulus ERP noise was not significantly test-retest reliable between electrode types for either condition (all  $r$ 's  $< 0.4$ , all  $p$ 's  $> .35$ ). SNR correlations were also found to be significantly correlated

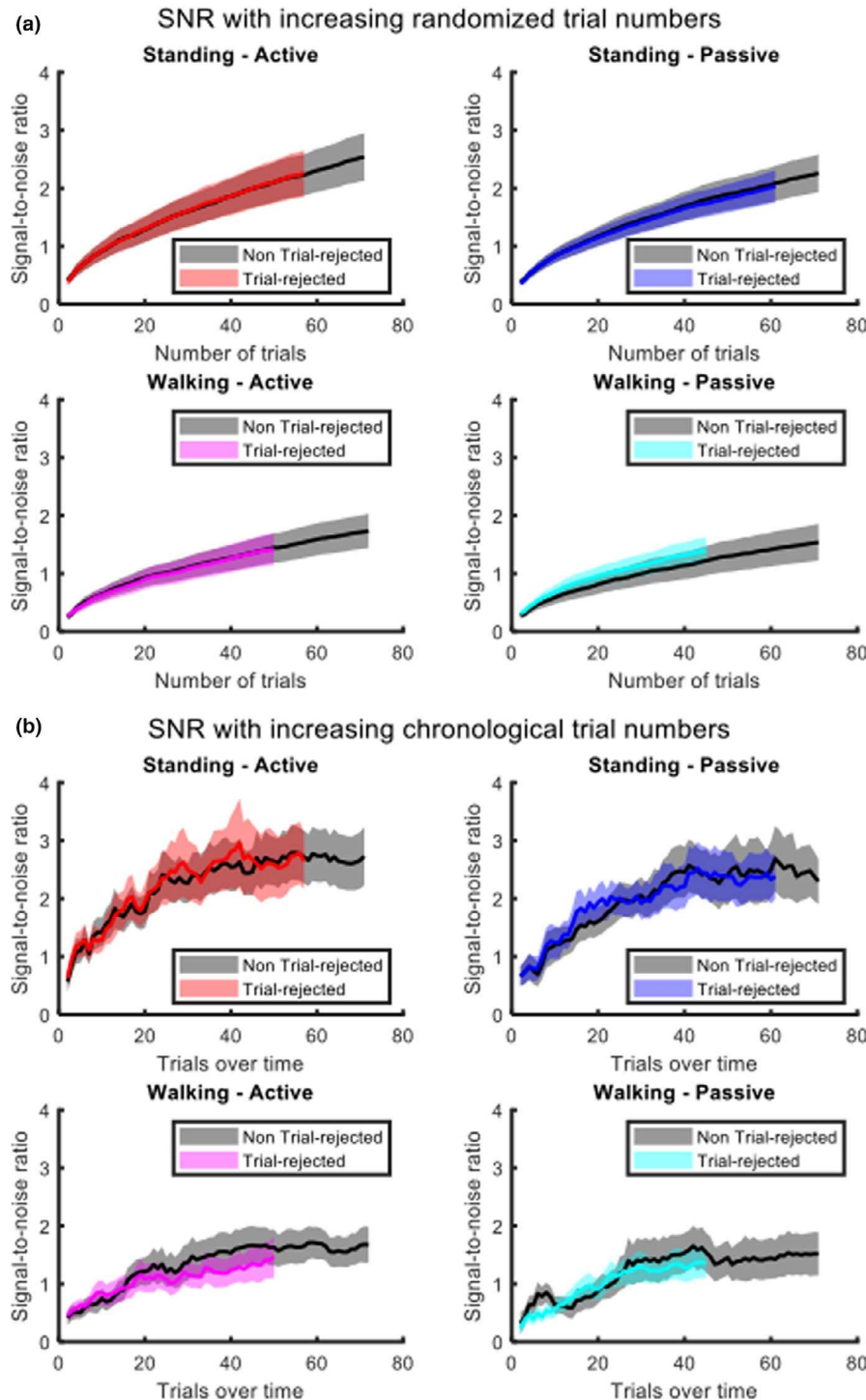


**FIGURE 4** Signal-to-noise ratio plotted as a function of increased trial numbers. (a) Signal-to-noise ratio as a function of increasing trial numbers for trial-rejected and non-trial rejected datasets within each condition. Effects of time were removed using 100 permutations of all trials for each number of trials. (b) Signal-to-noise ratio as a function of increasing chronological trial numbers for trial-rejected and non-trial rejected datasets within each condition. In both plots, data are plotted until the minimum trial number (the number of trials for the subject with the fewest trials) in each condition

between electrodes in the *walking* ( $r = 0.53, p = .022; pi = 0.63, p = .020$ ) but not *standing* ( $r = 0.51, p = .032; pi = 0.53; p = .088$ ) conditions after outlier removal. This illustrated a strong correlation in each condition (Cohen, 1992, 2013), with 28% and 26% shared variance ( $R^2$ ) in the *standing* and *walking* conditions between electrode types, respectively. Additionally, the P3 amplitude was found to be significantly test-retest reliable between electrode types during the *walking* ( $r = 0.67, p = .0021; pi = 0.65, p < .022$ ; Figure 5) but not the *standing* condition ( $r = 0.69, p = .0016;$

$pi = 0.62, p = .023$ ; Figure 5). The walking condition demonstrated a strong correlation (Cohen, 1992, 2013) with 45% shared variance.

## 4 | DISCUSSION

Mobile EEG typically is performed using a configuration made for active- or passive-transmission electrodes. Several claims have been made about the benefits of pre-amplification

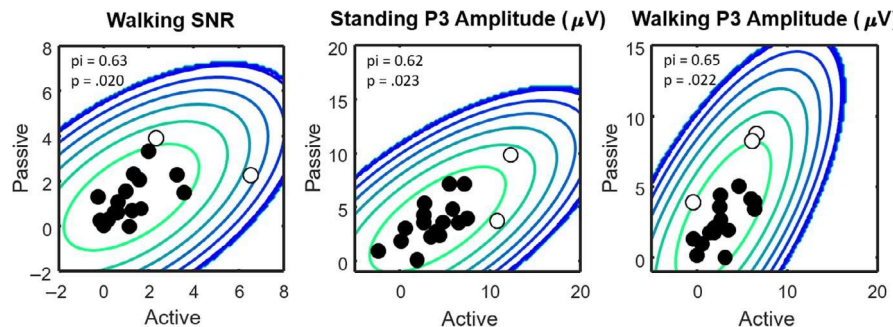


**FIGURE 5** Retest reliability. Test-retest reliability computed for walking condition signal-to-noise ratio (SNR), standing condition P3 amplitude, and walking condition P3 amplitude. The contour lines indicate bootstrapped Mahalanobis distance in steps of six squared units (darker shades denote greater distances). Open circles indicate outliers

directly on the head used by active electrodes for mobile EEG (Laszlo et al., 2014; Xu et al., 2017), but few studies have performed any direct comparison to a passive electrode configuration which also features amplification directly at the head during movement. The current study used typical active and passive electrode configurations with the same amplifier to record EEG data during an auditory oddball task, while participants were either *standing* or *walking* outdoors. We predicted that the P3 would be reduced during *walking*, and confirmed this hypothesis. We expected data quality to be reduced in the *walking* condition, and this was confirmed with reduced SNR and trial numbers. However, we found no evidence in support of our third hypothesis, as the typical *active* and *passive* electrode configurations performed equally well when collecting data for the same mobile task. We were able to collect proper ERP waveforms and demonstrate, like many previous studies, that the P3 can be reliably captured during a mobile task, regardless of active or passive electrode configuration (De Vos, Gandras, et al., 2014; De Vos, Kroesen, et al., 2014; Debener et al., 2012; Ladouce et al., 2019; Scanlon et al., 2019; Zink et al., 2016). Additionally, we were able to demonstrate, similar to previous work (Oliveira et al., 2016a, 2016b), that trait-like individual differences in noise and brain activity during walking are robust enough to even tolerate different electrode systems on different days.

#### 4.1 | P3 amplitude

Both electrode types were able to record ERPs (Figure 2), while both *standing* and *walking*, with no significant difference between electrode systems in either mobility condition. In agreement with previous studies (De Vos, Gandras, et al., 2014; De Vos, Kroesen, et al., 2014; Debener et al., 2012; Ladouce et al., 2019), we demonstrated a reduction in the P3 response to target trials during walking. The Bayesian ANOVA confirmed these results, indicating that the P3 reduction during *walking* was approximately equivalent between electrode types. It is likely that the P3 reduction is not simply driven by more noise

in the mobile condition. Rather it seems to reflect differences in cognitive demands in mobile versus stationary conditions, hence the reduction of the P3 amplitude for the primary, oddball task (Polich, 1987; Polich & Kok, 1995). The relationship between ERPs and motor activity may also be rooted in the inhibitory effect of the motor system on the auditory cortex (Nelson et al., 2013; Nordin et al., 2019a, 2019b, 2019c; Otazu et al., 2009; Schneider et al., 2014). Studies of freely behaving mice have shown that excitatory neurons within the auditory cortex may be postsynaptically inhibited by movement, demonstrating a mechanism for the suppression of auditory-evoked potentials during motor activity (Nordin et al., 2019b; Otazu et al., 2009; Schneider et al., 2014). Before and during movement, duplicate motor signals are sent into sensory pathways which aid one's interpretation of sensations being either self-induced sensory feedback due to motion or external unexpected stimuli (Crapse & Sommer, 2008; Martikainen et al., 2005; Nordin et al., 2019b; Poulet & Hedwig, 2006). Therefore, suppressed electrocortical responses such as the P3 during movement could be due to increased sensory feedback and motor activity. This has been shown to be relative to the amount of movement, as studies by Nordin et al. (2019a, 2019b, 2019c) have demonstrated decreases in the N1, P3, and alpha and beta spectral power with increased gait speeds. In our study, the trend of decreased P3 amplitude during walking was clear for both electrode types (Figure 2). Additionally, we were able to show that the P3 response was test-retest reliable, despite the use of different electrode configurations on different days. This indicates, similar to previous studies (De Vos, Gandras, et al., 2014; De Vos, Kroesen, et al., 2014; Debener et al., 2012; Zink et al., 2016), that the P3 is somewhat unique to individuals, and that variance contributed by electrode systems did not mask trait-like individual differences in P3 amplitude.

#### 4.2 | Trial numbers

We investigated the number of trials that remained after artifact processing as an additional estimate of data noise before

trial-rejection. We found that on average, there was no difference in trial numbers between electrode types, but a significant decrease in the number of remaining trials after artifact attenuation in the walking condition. This was expected, as similar results were found by Oliveira et al. (2016a, 2016b), and because the movement can increase data noise and artifacts (Debener et al., 2012; Gramann et al., 2010; Oliveira et al., 2016a, 2016b; Scanlon et al., 2019; Zink et al., 2016), leading to a higher probability of rejecting trials during movement. However, trial numbers following trial rejection are enough to properly record the P3 in each condition (Table 1; Luck, 2005a, 2005b).

#### 4.3 | Prestimulus ERP baseline noise

Data noise measured in the prestimulus ERP baseline at Pz was shown to be slightly increased due to walking for both electrode types (Figure 3), similar to previous mobile EEG studies with movement (Gramann et al., 2010; Oliveira et al., 2016a, 2016b; Scanlon et al., 2019). While this difference did not reach significance in the ANOVA, the Bayesian ANOVA indicated evidence for this main effect. It is possible this difference was small due to the noise being removed through ERP averaging (Luck, 2014). The ability of ERP averaging to remove noise that is not locked to the signal is one of the reasons that the oddball task and other ERP tasks are very popular within mobile EEG literature. There was also no main effect or interaction involving the electrode system, indicating that the electrode system did not have an effect on the prestimulus ERP baseline noise. The Bayesian ANOVA then confirmed that after artifact rejection, both electrode configurations were equally affected by increases in noise caused by walking.

#### 4.4 | Signal-to-noise ratio

Similar to previous studies (Debener et al., 2012; Oliveira et al., 2016a, 2016b), SNR was shown to be decreased for both electrode systems during the walking conditions. Similar to prestimulus ERP data noise, there was no effect of the electrode type or interaction. These results were then confirmed by the Bayesian ANOVA. SNR is calculated using both the P3 amplitude and data noise, and therefore, this result is likely due to a combination of both decreased P3 amplitude and increased data noise during walking.

The trial rejection analysis confirmed that trial rejection did not significantly change the SNR when analyzed chronologically. However, when analyzing the SNR non-chronologically, the final SNR was smaller in the trial-rejected than the non-trial rejected data (Figure 4a). This could simply be due to the larger number of trials before trial-rejection as the

slopes of the SNR over time appear similar in both datasets. The difference between the chronological and non-chronological SNR demonstrates two specific questions that mobile EEG researchers often face when designing experiments. These are: “how much data do I need?” and, “how long do I need to record my data?”. The first question is somewhat answered by the permutational analysis of SNR data using more trials at each iteration. When the confound of time is removed it appears that more data are always better, even when some trials contain artifacts. Indeed, artifacts here may even increase the SNR, as blinks or movement artifacts may even demonstrate higher amplitudes than that of the P3. The second question then, for this study, is answered by the analysis of SNR as trials increase over time (Figure 4b). Evident from the plots, without the permutations of trials in time, the non-trial rejected data do not have any advantage with respect to SNR, even with significantly more trials. This may be because over time, humans habituate to stimuli (Polich, 1989; Polich & Kok, 1995), lose interest in the task (Kok, 2001), or signal quality may decrease (e.g. electrodes may lose contact or dry out). Again, here we found no effect of the electrode configuration, demonstrating that the performance of the chosen active and passive configurations did not differ on any measure of SNR in this study.

#### 4.5 | Retest reliability analyses

Test-retest reliability gives an estimate of how much the inter-subject variability is consistent over time and using different electrode systems, and also provides an additional estimate of effect size (Baugh, 2002). This testing differs somewhat from the usual test-retest measurement, which often consists of performing the same test in the same conditions. However, our purpose here was to compare for similarities between the two configurations, not to test the effectiveness of the mobile systems themselves, as the effectiveness of mobile data recording has been previously validated (De Vos, Gandras, et al., 2014; De Vos, Kroesen, et al., 2014; Oliveira et al., 2016a, 2016b; Scanlon et al., 2019). We found significant test-retest reliabilities between electrode configurations for the measures of SNR and P3 amplitude. While it has long been known that most physiological signals, such as ERP patterns, tend to vary more between individuals than within (Luck, 2014), this was also found for SNR. Test-retest reliability in P3 (De Vos, Gandras, et al., 2014; De Vos, Kroesen, et al., 2014; Debener et al., 2012) and SNR has been demonstrated for a mobile task within electrode types before (Oliveira et al., 2016a, 2016b); however, to our knowledge, this is the first time these measures have been tested for test-retest reliability using different electrode systems on different days. In particular, average SNR values were found to be correlated between electrode types in the walking condition,

indicating that some participants consistently have noisier data than others, regardless of electrode type or possible day by day differences in cap application or impedance reduction. These individual differences could come from a variety of factors, such as hair thickness, individual walking patterns or posture.

## 4.6 | Limitations

In this study we attempted to keep all factors equal between two electrode signal-transmission configurations; however, some factors we were not able to control. The passive electrode system was designed following our experience with head-mounted wireless EEG systems such as Emotiv ([www.emotiv.com](http://www.emotiv.com)) and SMARTING (mBrainTrain, 183 Belgrade, Serbia; Daeglau et al., 2020; Debener et al., 2012) and therefore had short wires. The active system, moreover, was used with longer wires, which allowed placing amplifiers in a backpack. This was performed in accordance with the manufacturer's recommendations for active electrodes (Brain Products GmbH, 2019) as well as with previous experiences with active electrode mobile EEG systems (Scanlon et al., 2017, 2019, 2020). While we have not directly tested this in the present study, it should be clear that wire movements must be heavily controlled when passive electrodes are used. This can be achieved by keeping wires bundled together and as short as possible, hence the requirement of head-mounted and wireless amplifiers. To the authors' knowledge, no similar study has been published reporting exactly the detrimental effect of wire length and movement on EEG acquisition with passive electrodes, but a few studies have reported motion artifact within active electrodes with high frequencies of cable sway (Nathan & Contreras-Vidal, 2016; Peterson & Ferris, 2019; Symeonidou et al., 2018). While this study puts an emphasis on ecological validity and real-world EEG acquisition, several studies have made progress in artifact measurement and removal by isolating artifactual signals through the use of phantom-head designs (Nordin et al., 2018, 2019a, 2019b, 2019c; Oliveira et al., 2016a, 2016b; Richer et al., 2019; Ries et al., 2014).

The results of this study were drawn from ERP analysis, which has an additional processing advantage of being able to decrease the effects of extraneous and non-time-locked noise simply through averaging (Luck, 2014). To what extent they can be generalized to other types of EEG analysis remains to be determined.

## 4.7 | Conclusions

With adequate set-up and preprocessing, both active and passive electrode configurations can be used to collect

mobile EEG data. For future advances in mobile EEG research, it would be beneficial to use high-density, lightweight, and miniaturized EEG systems that keep all wires short and bundled and wirelessly stream signals to a portable acquisition unit. It appears especially important to include some amplification that takes place directly on the head, regardless of whether this is pre-amplification in the electrodes or simple amplification in an amplifier. For real-life applications, such systems might incorporate transparent EEG design concepts (Bleichner & Debener, 2017). It seems less important to us whether active or passive electrodes are included.

## ACKNOWLEDGMENTS

This work was supported by an NSERC PGSD research grant to JEMS.

## CONFLICT OF INTEREST

The authors declare no competing financial interests.

## AUTHOR CONTRIBUTIONS

JEMS, NSJJ, MCM, and SD piloted and designed the experiment. MCM and JEMS set-up and performed the experiments. JEMS, SD and NSJJ analyzed and interpreted the data. JEMS and SD drafted the manuscript, and all authors edited and approved the final version.

## PEER REVIEW

The peer review history for this article is available at <https://publons.com/publon/10.1111/ejn.15037>.

## DATA AVAILABILITY STATEMENT

Data for this article have been documented according to the EEG Study Scheme standard ([www.eegstudy.org](http://www.eegstudy.org)) and are available upon request (joanna.elizabeth.mary.scanlon@uni-oldenburg.de).

## ORCID

*Joanna E. M. Scanlon*  <https://orcid.org/0000-0001-8561-9088>

*Nadine Svenja Josée Jacobsen*  <https://orcid.org/0000-0001-6612-7328>

## REFERENCES

- Abdi, H. (2010). Holm's sequential Bonferroni procedure. *Encyclopedia of Research Design*, 1(8), 1–8.
- Baugh, F. (2002). Correcting effect sizes for score reliability: A reminder that measurement and substantive issues are linked inextricably. *Educational and Psychological Measurement*, 62(2), 254–263. <https://doi.org/10.1177/0013164402062002004>
- Bleichner, M. G., & Debener, S. (2017). Concealed, unobtrusive ear-centered EEG acquisition: cEEGGrids for transparent EEG. *Frontiers in Human Neuroscience*, 11, 163. <https://doi.org/10.3389/fnhum.2017.00163>

- Boudewyn, M. A., Luck, S. J., Farrens, J. L., & Kappenman, E. S. (2018). How many trials does it take to get a significant ERP effect? It depends. *Psychophysiology*, 55(6), e13049. <https://doi.org/10.1111/psyp.13049>
- Brain Products GmbH. (2019, Aug 20). *LiveAmp operating instructions*. Retrieved from <https://www.brainproducts.com/downloads.php?kid=5&dlspath=Manuals>
- Chan, M., Nyazika, S., & Singhal, A. (2016). Effects of a front-seat passenger on driver attention: An electrophysiological approach. *Transportation Research Part F: Traffic Psychology and Behaviour*, 43, 67–79. <https://doi.org/10.1016/j.trf.2016.09.016>
- Cohen, J. (1992). A power primer. *Psychological Bulletin*, 112(1), 155. <https://doi.org/10.1037/0033-2909.112.1.155>
- Cohen, J. (2013). *Statistical power analysis for the behavioral sciences*. Academic press.
- Crapse, T. B., & Sommer, M. A. (2008). Corollary discharge across the animal kingdom. *Nature Reviews Neuroscience*, 9(8), 587–600. <https://doi.org/10.1038/nrn2457>
- Daeglaeu, M., Wallhoff, F., Debener, S., Condro, I. S., Kranczioch, C., & Zich, C. (2020). Challenge accepted? Individual performance gains for motor imagery practice with humanoid robotic EEG neurofeedback. *Sensors*, 20(6), 1620. <https://doi.org/10.3390/s20061620>
- De Vos, M., Gandras, K., & Debener, S. (2014). Towards a truly mobile auditory brain–computer interface: Exploring the P300 to take away. *International Journal of Psychophysiology*, 91(1), 46–53.
- De Vos, M., Kroesen, M., Emkes, R., & Debener, S. (2014). P300 speller BCI with a mobile EEG system: Comparison to a traditional amplifier. *Journal of Neural Engineering*, 11(3), 036008.
- Debener, S., Minow, F., Emkes, R., Gandras, K., & De Vos, M. (2012). How about taking a low-cost, small, and wireless EEG for a walk? *Psychophysiology*, 49(11), 1617–1621.
- Debener, S., Strobel, A., Sorger, B., Peters, J., Kranczioch, C., Engel, A. K., & Goebel, R. (2007). Improved quality of auditory event-related potentials recorded simultaneously with 3-T fMRI: Removal of the ballistocardiogram artefact. *NeuroImage*, 34(2), 587–597.
- Delorme, A., & Makeig, S. (2004). EEGLAB: An open source toolbox for analysis of single-trial EEG dynamics including independent component analysis. *Journal of Neuroscience Methods*, 134(1), 9–21.
- Finneran, J. J., Mulsow, J., & Burkard, R. F. (2019). Signal-to-noise ratio of auditory brainstem responses (ABRs) across click rate in the bottlenose dolphin (*Tursiops truncatus*). *The Journal of the Acoustical Society of America*, 145(2), 1143–1151.
- Gramann, K., Gwin, J. T., Bigdely-Shamlo, N., Ferris, D. P., & Makeig, S. (2010). Visual evoked responses during standing and walking. *Frontiers in Human Neuroscience*, 4, 202.
- Gratton, G., Coles, M. G., & Donchin, E. (1983). A new method for off-line removal of ocular artifact. *Electroencephalography and Clinical Neurophysiology*, 55(4), 468–484.
- Gwin, J. T., Gramann, K., Makeig, S., & Ferris, D. P. (2010). Removal of movement artifact from high-density EEG recorded during walking and running. *Journal of Neurophysiology*, 103(6), 3526–3534.
- Holm, S. (1979). A simple sequentially rejective multiple test procedure. *Scandinavian Journal of Statistics*, 65–70.
- JASP Team (2020). JASP (Version 0.12.2) [Computer software].
- Jung, T. P., Makeig, S., Westerfield, M., Townsend, J., Courchesne, E., & Sejnowski, T. J. (2000). Removal of eye activity artifacts from visual event-related potentials in normal and clinical subjects. *Clinical Neurophysiology*, 111(10), 1745–1758. [https://doi.org/10.1016/S1388-2457\(00\)00386-2](https://doi.org/10.1016/S1388-2457(00)00386-2)
- Kam, J. W. Y., Griffin, S., Shen, A., Patel, S., Hinrichs, H., Heinze, H.-J., Deouell, L. Y., & Knight, R. T. (2019). Systematic comparison between a wireless EEG system with dry electrodes and a wired EEG system with wet electrodes. *NeuroImage*, 184, 119–129. <https://doi.org/10.1016/j.neuroimage.2018.09.012>
- Kappenman, E. S., & Luck, S. J. (2010). The effects of electrode impedance on data quality and statistical significance in ERP recordings. *Psychophysiology*, 47(5), 888–904.
- Keil, A., Debener, S., Gratton, G., Junghöfer, M., Kappenman, E. S., Luck, S. J., Luu, P., Miller, G. A., & Yee, C. M. (2014). Committee report: Publication guidelines and recommendations for studies using electroencephalography and magnetoencephalography. *Psychophysiology*, 51(1), 1–21. <https://doi.org/10.1111/psyp.12147>
- Kelly, J. P., Darvas, F., & Weiss, A. H. (2014). Waveform variance and latency jitter of the visual evoked potential in childhood. *Documenta Ophthalmologica*, 128(1), 1–12.
- Kok, A. (2001). On the utility of P3 amplitude as a measure of processing capacity. *Psychophysiology*, 38(3), 557–577. <https://doi.org/10.1017/S0048577201990559>
- Kremláček, J., Hulan, M., Kuba, M., Kubová, Z., Langrová, J., Vit, F., & Szanyi, J. (2012). Role of latency jittering correction in motion-onset VEP amplitude decay during prolonged visual stimulation. *Documenta Ophthalmologica*, 124(3), 211–223.
- Ladouce, S., Donaldson, D. I., Dudchenko, P. A., & Ietswaart, M. (2019). Mobile EEG identifies the re-allocation of attention during real-world activity. *Scientific Reports*, 9(1), 1–10. <https://doi.org/10.1038/s41598-019-51996-y>
- Laszlo, S., Ruiz-Blondet, M., Khalifian, N., Chu, F., & Jin, Z. (2014). A direct comparison of active and passive amplification electrodes in the same amplifier system. *Journal of Neuroscience Methods*, 235, 298–307. <https://doi.org/10.1016/j.jneumeth.2014.05.012>
- Luck, S. J. (2005a). *An introduction to the event-related potential technique: Cognitive neuroscience*.
- Luck, S. J. (2005b). *Ten simple rules for designing ERP experiments. Event-related potentials: A methods handbook* (p. 262083337). MIT press.
- Luck, S. J. (2014). *An introduction to the event-related potential technique* (p. 683). MIT Press.
- Marini, F., Lee, C., Wagner, J., Makeig, S., & Gola, M. (2019). A comparative evaluation of signal quality between a research-grade and a wireless dry-electrode mobile EEG system. *Journal of Neural Engineering*, 16(5), 054001.
- Martikainen, M. H., Kaneko, K. I., & Hari, R. (2005). Suppressed responses to self-triggered sounds in the human auditory cortex. *Cerebral Cortex*, 15(3), 299–302.
- Mathewson, K. E., Harrison, T. J., & Kizuk, S. A. (2017). High and dry? Comparing active dry EEG electrodes to active and passive wet electrodes. *Psychophysiology*, 54(1), 74–82.
- MATLAB. (2016). Version 1.7.0\_60 (R2016a). The MathWorks Inc.
- Mega Electronics. (2017, April). 800778 eMotion Faros Series Manual. Retrieved from <https://ecgcloud.co.uk/software/8007782.3.0%20eMotion%20Faros%20Series%20Manual.pdf>
- Nathan, K., & Contreras-Vidal, J. L. (2016). Negligible motion artifacts in scalp electroencephalography (EEG) during treadmill walking. *Frontiers in Human Neuroscience*, 9, 708.
- Nelson, A., Schneider, D. M., Takatoh, J., Sakurai, K., Wang, F., & Mooney, R. (2013). A circuit for motor cortical modulation

- of auditory cortical activity. *Journal of Neuroscience*, 33(36), 14342–14353.
- Nordin, A. D., Hairston, W. D., & Ferris, D. P. (2018). Dual-electrode motion artifact cancellation for mobile electroencephalography. *Journal of Neural Engineering*, 15(5), 056024. <https://doi.org/10.1088/1741-2552/aad7d7>
- Nordin, A. D., Hairston, W. D., & Ferris, D. P. (2019a). Faster gait speeds reduce alpha and beta EEG spectral power from human sensorimotor cortex. *IEEE Transactions on Biomedical Engineering*, 67(3), 842–853.
- Nordin, A. D., Hairston, W. D., & Ferris, D. P. (2019b, October). Faster gait speeds suppress human auditory electrocortical responses. In *2019 IEEE International Conference on Systems, Man and Cybernetics (SMC)* (pp. 235–240). IEEE. <https://www.sciencegate.app/doi/abs/10.1109/tbme.2020.2977756>
- Nordin, A. D., Hairston, W. D., & Ferris, D. P. (2019c). Human electrocortical dynamics while stepping over obstacles. *Scientific Reports*, 9(1), 1–12. <https://doi.org/10.1038/s41598-019-41131-2>
- Oliveira, A. S., Schlink, B. R., Hairston, W. D., König, P., & Ferris, D. P. (2016a). Induction and separation of motion artifacts in EEG data using a mobile phantom head device. *Journal of Neural Engineering*, 13(3), 036014. <https://doi.org/10.1088/1741-2560/13/3/036014>
- Oliveira, A. S., Schlink, B. R., Hairston, W. D., König, P., & Ferris, D. P. (2016b). Proposing metrics for benchmarking novel EEG technologies towards real-world measurements. *Frontiers in Human Neuroscience*, 10, 188. <https://doi.org/10.3389/fnhum.2016.00188>
- Otazu, G. H., Tai, L. H., Yang, Y., & Zador, A. M. (2009). Engaging in an auditory task suppresses responses in auditory cortex. *Nature Neuroscience*, 12(5), 646. <https://doi.org/10.1038/nn.2306>
- Peterson, S. M., & Ferris, D. P. (2019). Combined head phantom and neural mass model validation of effective connectivity measures. *Journal of Neural Engineering*, 16(2), 026010. <https://doi.org/10.1088/1741-2552/aaf60e>
- Pion-Tonachini, L., Kreutz-Delgado, K., & Makeig, S. (2019). ICLLabel: An automated electroencephalographic independent component classifier, dataset, and website. *NeuroImage*, 198, 181–197. <https://doi.org/10.1016/j.neuroimage.2019.05.026>
- Polich, J. (1987). Task difficulty, probability, and inter-stimulus interval as determinants of P300 from auditory stimuli. *Electroencephalography and Clinical Neurophysiology/Evoked Potentials Section*, 68(4), 311–320. [https://doi.org/10.1016/0168-5597\(87\)90052-9](https://doi.org/10.1016/0168-5597(87)90052-9)
- Polich, J. (1989). Habituation of P300 from auditory stimuli. *Psychobiology*, 17(1), 19–28.
- Polich, J., & Kok, A. (1995). Cognitive and biological determinants of P300: An integrative review. *Biological Psychology*, 41(2), 103–146.
- Poulet, J. F., & Hedwig, B. (2006). The cellular basis of a corollary discharge. *Science*, 311(5760), 518–522.
- Richer, N., Downey, R. J., Nordin, A. D., Hairston, W. D., & Ferris, D. P. (2019, March). Adding neck muscle activity to a head phantom device to validate mobile EEG muscle and motion artifact removal. In J. Carmen & P. Sajda (Eds.), *2019 9th International IEEE/EMBS Conference on Neural Engineering (NER)* (pp. 275–278). IEEE. <http://worldcat.org/identities/lccn-no2003036080/>
- Ries, A. J., Touryan, J., Vettel, J., McDowell, K., & Hairston, W. D. (2014). A comparison of electroencephalography signals acquired from conventional and mobile systems. *Journal of Neuroscience and Neuroengineering*, 3(1), 10–20.
- Scanlon, J. E. M., Redman, E. X., Kuziek, J. W., & Mathewson, K. E. (2020). A ride in the park: Cycling in different outdoor environments modulates the auditory evoked potentials. *International Journal of Psychophysiology*, 151, 59–69.
- Scanlon, J. E., Sieben, A. J., Holyk, K. R., & Mathewson, K. E. (2017). Your brain on bikes: P3, MMN/N2b, and baseline noise while pedaling a stationary bike. *Psychophysiology*, 54(6), 927–937.
- Scanlon, J. E. M., Townsend, K. A., Cormier, D. L., Kuziek, J. W., & Mathewson, K. E. (2019). Taking off the training wheels: Measuring auditory P3 during outdoor cycling using an active wet EEG system. *Brain Research*, 1716, 50–61.
- Schimmel, H. (1967). The ( $\pm$ ) reference: Accuracy of estimated mean components in average response studies. *Science*, 157(3784), 92–94.
- Schneider, D. M., Nelson, A., & Mooney, R. (2014). A synaptic and circuit basis for corollary discharge in the auditory cortex. *Nature*, 513(7517), 189–194.
- Schwarzkopf, D. S., De Haas, B., & Rees, G. (2012). Better ways to improve standards in brain-behavior correlation analysis. *Frontiers in Human Neuroscience*, 6, 200.
- Symeonidou, E. R., Nordin, A. D., Hairston, W. D., & Ferris, D. P. (2018). Effects of cable sway, electrode surface area, and electrode mass on electroencephalography signal quality during motion. *Sensors*, 18(4), 1073. <https://doi.org/10.3390/s18041073>
- Viola, F. C., Thorne, J., Edmonds, B., Schneider, T., Eichele, T., & Debener, S. (2009). Semi-automatic identification of independent components representing EEG artifact. *Clinical Neurophysiology*, 120(5), 868–877. <https://doi.org/10.1016/j.clinph.2009.01.015>
- Wright, T. J., Nilsson, J., & Westall, C. (2011). Isolating Visual Evoked Responses—Comparing Signal Identification Algorithms. *Journal of Clinical Neurophysiology*, 28(4), 404–411. <https://doi.org/10.1097/WNP.0b013e3182273351>
- Xu, J., Mitra, S., Van Hoof, C., Yazicioglu, R. F., & Makinwa, K. A. (2017). Active electrodes for wearable EEG acquisition: Review and electronics design methodology. *IEEE Reviews in Biomedical Engineering*, 10, 187–198. <https://doi.org/10.1109/RBME.2017.2656388>
- Zink, R., Hunyadi, B., Van Huffel, S., & De Vos, M. (2016). Mobile EEG on the bike: Disentangling attentional and physical contributions to auditory attention tasks. *Journal of Neural Engineering*, 13(4), 046017. <https://doi.org/10.1088/1741-2560/13/4/046017>

**How to cite this article:** Scanlon JEM, Jacobsen NSJ, Maack MC, Debener S. Does the electrode amplification style matter? A comparison of active and passive EEG system configurations during standing and walking. *Eur J Neurosci*. 2020;00:1–15. <https://doi.org/10.1111/ejn.15037>